Clays and Clay Minerals, Vol. 45, No. 3, 378–389, 1997.

TEXTURAL TRANSITION AND GENETIC RELATIONSHIP BETWEEN PRECURSOR STEVENSITE AND SEPIOLITE IN LACUSTRINE SEDIMENTS (JBEL RHASSOUL, MOROCCO)

AZEDDINE CHAHI,[1,3] BERTRAND FRITZ,[1] JOELLE DUPLAY,[1] FRANCIS WEBER[1] AND JACQUES LUCAS[1,2]

[1] Centre de Géochimie de la Surface, CNRS, 1, rue Blessig, 67084 Strasbourg Cedex, France

[2] Université Louis Pasteur, Institut des Sciences de la terre, 1, rue Blessig, 67084 Strasbourg Cedex, France

[3] Faculté des Sciences Semlalia, Boulevard Amir Moulay Abdellah, BP S.15 Marrakech, Maroc

Abstract—In the Tertiary lacustrine sediments of the Jbel Rhassoul (Morocco), stevensite and sepiolite, confined to the dolomitic facies, are commonly mixed at lower parts of the so-called "Formation Intermédiaire". Transmission electron microscopy (TEM) observations reveal a relation between these 2 magnesian clay minerals. One can observe the different transition steps, from the initial folded layers of stevensite to the fibers emerging from the layers, and finally to the complete replacement of stevensite by sepiolite. That transition can also be observed by scanning electron microscopy (SEM), where the fibers seem to grow at the expense of stevensite. Thermodynamic calculations have been applied to provide geochemical conditions for the formation of sepiolite after stevensite. Early deposition of the "Formation Intermédiaire" occurred under climatic conditions varying between dry and wet. During dry periods, the relative silica enrichment and the pH decrease in the lake water should destabilize stevensite, leading to the formation of sepiolite. Subsequently, a perennial wet climate would lead to the formation of pure stevensite without any trace of sepiolite.

Key Words—Jbel Rhassoul, Sepiolite, Stevensite, Textural Transition, Thermodynamic Calculation.

INTRODUCTION

The clay minerals found in the Tertiary continental deposits of the Jbel Rhassoul (Morocco) are detrital phengite, illite and chlorite, and neoformed illite/smectite, palygorskite, stevensite and sepiolite. These clay minerals are confined in separate levels of the Jbel Rhassoul formations and are associated with different minerals. Except for sepiolite, the origin and evolution of clay minerals from Jbel Rhassoul has been previously documented (Chahi 1992; Chahi et al. 1992; Chahi, Duplay and Lucas 1993; Gauthier-Lafaye et al. 1993; Duringer et al. 1995; Chahi 1996). Thus, the aim of this study is to assess the formation process of the sepiolite, which is confined to the dolomitic facies and is commonly associated with the stevensite. This dolomitic environment is similar to typical environments of sepiolite genesis in lacustrine deposits (Parry and Reeves 1966; McLean et al. 1972; Papke 1972; Stoessell and Hay 1978; Hay and Stoessell 1984; Leguey et al. 1985). Our model for sepiolite genesis is then compared with other models for lacustrine sepiolite.

FIELD OCCURENCE AND SAMPLE LOCATION

The Jbel Rhassoul formation is located in a small mountain at the east side of the Middle Atlas, in the Moulouya Valley, Morocco (Figure 1). Different authors have studied the Mio-Pliocene deposits of the Jbel Rhassoul and have attributed a lacustrine origin to the sediments (Raynal 1952; Trauth 1977; Lucas and Prévôt 1976). Recently, according to Duringer et al. (1995), the Jbel Rhassoul sediments preserve evidence of 2 distinct sedimentary stages (Figure 2). The first and oldest stage consists of very large, well-developed coarse-grained deltas that prograded into an evaporitic playa lake under an arid to semi-arid climate. Marls and saline marly deposits ("Formation Rouge") contain detrital illite and chlorite and neoformed palygorskite, but no stevensite (Lucas and Prévôt 1976; Chahi, Duplay and Lucas 1993; Gauthier-Lafaye et al. 1993). The younger stage is a fan-delta complex that prograded into a fresh or brackish water lacustrine and perennial environment under a wet climate (Chahi et al. 1992; Duringer et al. 1995). Stevensite, sepiolite and chert are confined to the marly-dolomitic deposits ("Formation Intermédiaire"). The stevensite is pure at the upper part of the "Formation Intermédiaire" (Figure 3, right side) and mixed with sepiolite at the lower part just above the "Formation Rouge" (Figure 3, left side). Thus, sepiolite which occurs between the palygorskite-rich formation and the stevensite-rich formation could have formed under a climate varying between dry and wet.

Six representative specimens (6, 7, 8, 9, 10, 11) chosen for this study were sampled at different levels of the "Formation Intermédiaire" (Figure 3): samples 6, 7 and 8 at the bottom of the formation and samples 9, 10 and 11 at the top. They contain clays, dolomite, celestite, quartz and gypsum traces (Table 1). The clay is quantitatively dominant.

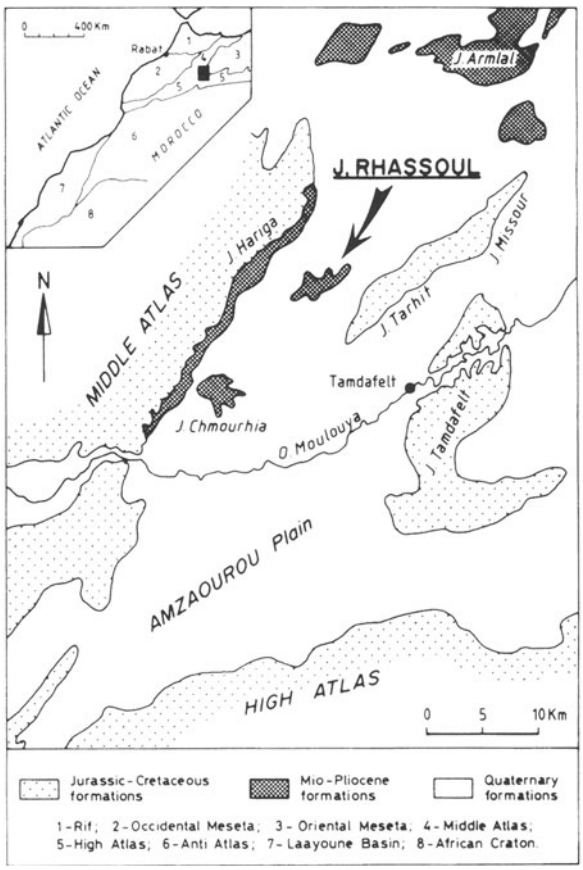

Figure 1. Location of the Jbel Rhassoul formations in Morocco.

EXPERIMENTAL METHODS

Sample Preparation

The samples contained sulfates and carbonates. Acid treatment of the <2 μm fraction was efficient in removing them, but destroyed the clay. Therefore, a method of treatment using cation exchange resins was chosen to remove carbonates and sulfates without damage to the clay minerals (Chahi, Weber et al. 1993). The resin, used at 60 °C, was Amberlite IRC-50H eluted with HCl (1.5 *N*). This treatment purifies and also results in good dispersion of the mineral suspension. When the amount of celestite was very important in the sample, either the Dowex 50WX4 eluted with HCl (1.5 *N*) (Chahi 1988), or the NaCl electrolyte was used for the purification of clay minerals.

X-ray Powder Diffraction (XRD) Analysis

XRD analysis was performed on nonoriented and oriented clays held at atmospheric conditions (N), on specimens saturated with ethylene glycol (E), and on samples heated at 490 °C for 4 h (H). Diffraction patterns were obtained for the <2 μm fraction in all samples.

Major and Trace Elements Analysis

Major elements have been analyzed by means of arc emission spectrometry. The relative error in the concentrations is around 2%. Trace elements have been analyzed by means of inductively coupled plasma emission spectrometry. The relative error in the concentrations is around 10% (Samuel et al. 1985).

Microscopy

Rock samples were observed by SEM (JEOL JSM 840). The TEM and high-resolution TEM (HRTEM) observations were made at 120 kV on a Philips CM12. The clays were diluted in pure water and treated in an ultrasonic device, and a drop of suspension was deposited on a carbon-coated copper grid. As sepiolite and stevensite are mixed in the sample, analytical electron microscopy (AEM) was particularly useful to determine the chemical composition of each species. This technique has already been successfully used for palygorskites (Chahi, Duplay and Lucas 1993) and stevensite (Duplay 1988) from the Jbel Rhassoul. Special care was taken to analyze individual particles or bundles of pure sepiolite fibers. Therefore, the clay suspension was

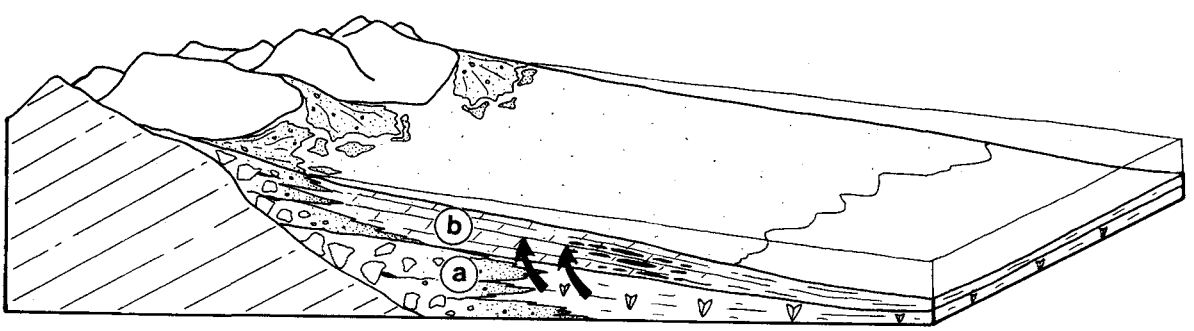

Figure 2. Geodynamic model for the formation of the Jbel Rhassoul and location of the worked deposit (black belts) and tardive migration of gypsum from lower fan-deltaic system (a) to upper fan-deltaic system (b) (Duringer et al. 1995).

https://doi.org/10.1346/CCMN.1997.0450308 Published online by Cambridge University Press

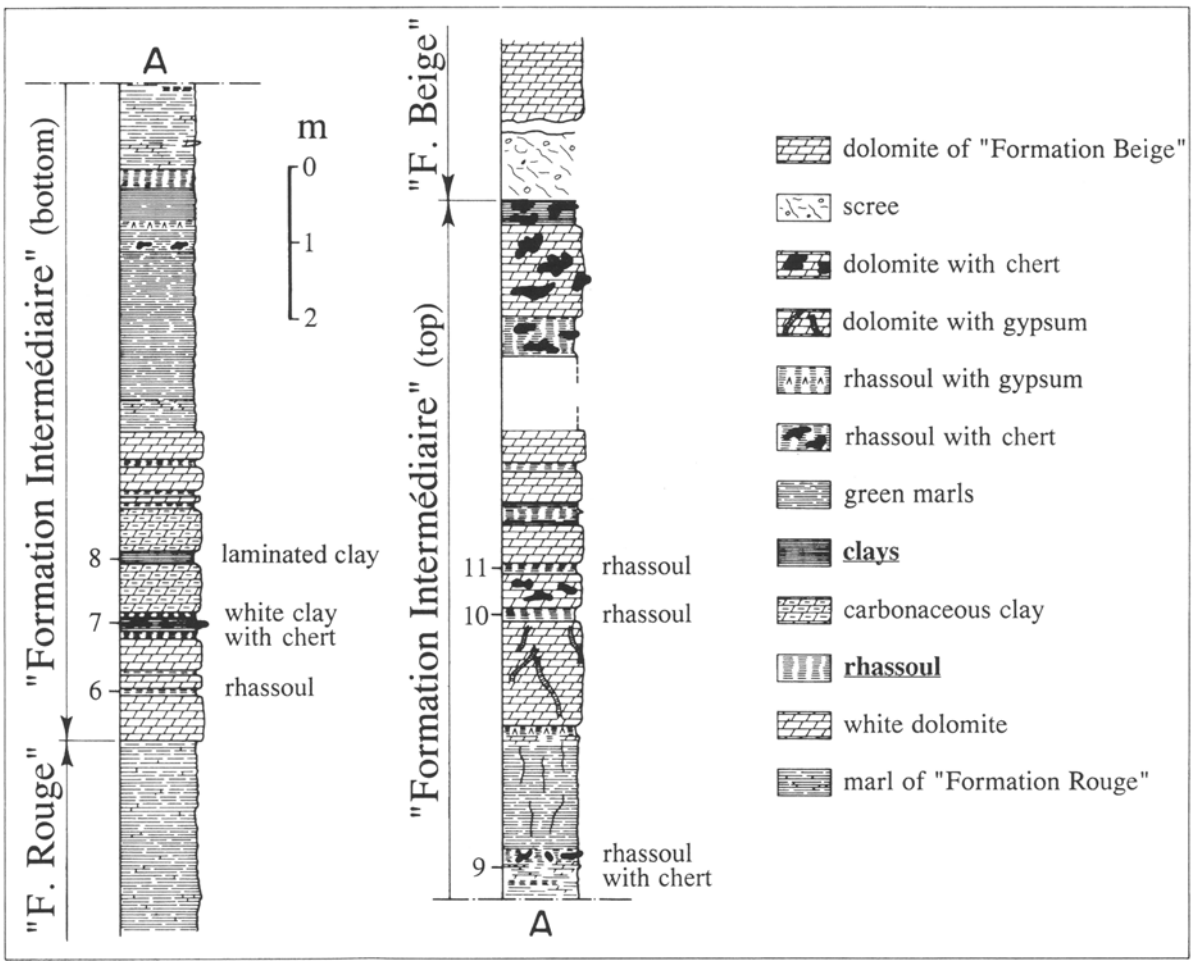

Figure 3. Location of the studied sample numbers in the "Formation Intermédiaire".

considerably diluted to avoid particle overlap. The analyses were performed by means of energy dispersive X-ray spectrometry (EDX) with an Si(Li) detector, and with the beam rastered over a small surface to avoid element diffusion (Peacor 1992). Quantitative results were obtained after corrections using a standard for thin films (phlogopite) and following the Cliff and Lorimer (1975) procedure. The estimated analytical errors in the concentrations are of the order of 2% for major elements, and 5 to 10% for minor elements.

In each sample, a population of stevensite particles as well as bundles of sepiolite fibers were analyzed. The structural formulae were calculated for half-unit cells, on the basis of 11 oxygens for stevensite and 23 for sepiolite. In AEM analyses it is neither possible to analyze Li nor to distinguish trivalent from divalent

Table 1. Semi-quantitative estimation of the mineralogical composition in the sediments of the "Formation Intermédiaire" from top (11) to bottom (6).

	Sample	Clay	Dolomite	Quartz	Celestite	Gypsum
Top	11	++++	—	—	—	tr
	10	++++	—	—	—	tr
	9	+++	+	tr	tr	tr
	8	++++	tr	tr	+	—
	7	++++	—	—	+	—
Bottom	6	+++	+	tr	+	tr

Key: ++++ (75–100%); +++ (50–75%); ++ (25–50%); + (<25%); tr: trace; — below detection limit.

Table 2. Semi-quantitative estimation of the clay species in the <2 μm fractions of the "Formation Intermédiaire".

Sample	Stevensite	Sepiolite
11	++++	—
10	++++	—
9	++++	—
8	++	+++
7	+	++++
6	+++	++

Key: ++++ (75–100%); +++ (50–75%); ++ (25–50%); + (<25%); — below detection limit.

https://doi.org/10.1346/CCMN.1997.0450308 Published online by Cambridge University Press

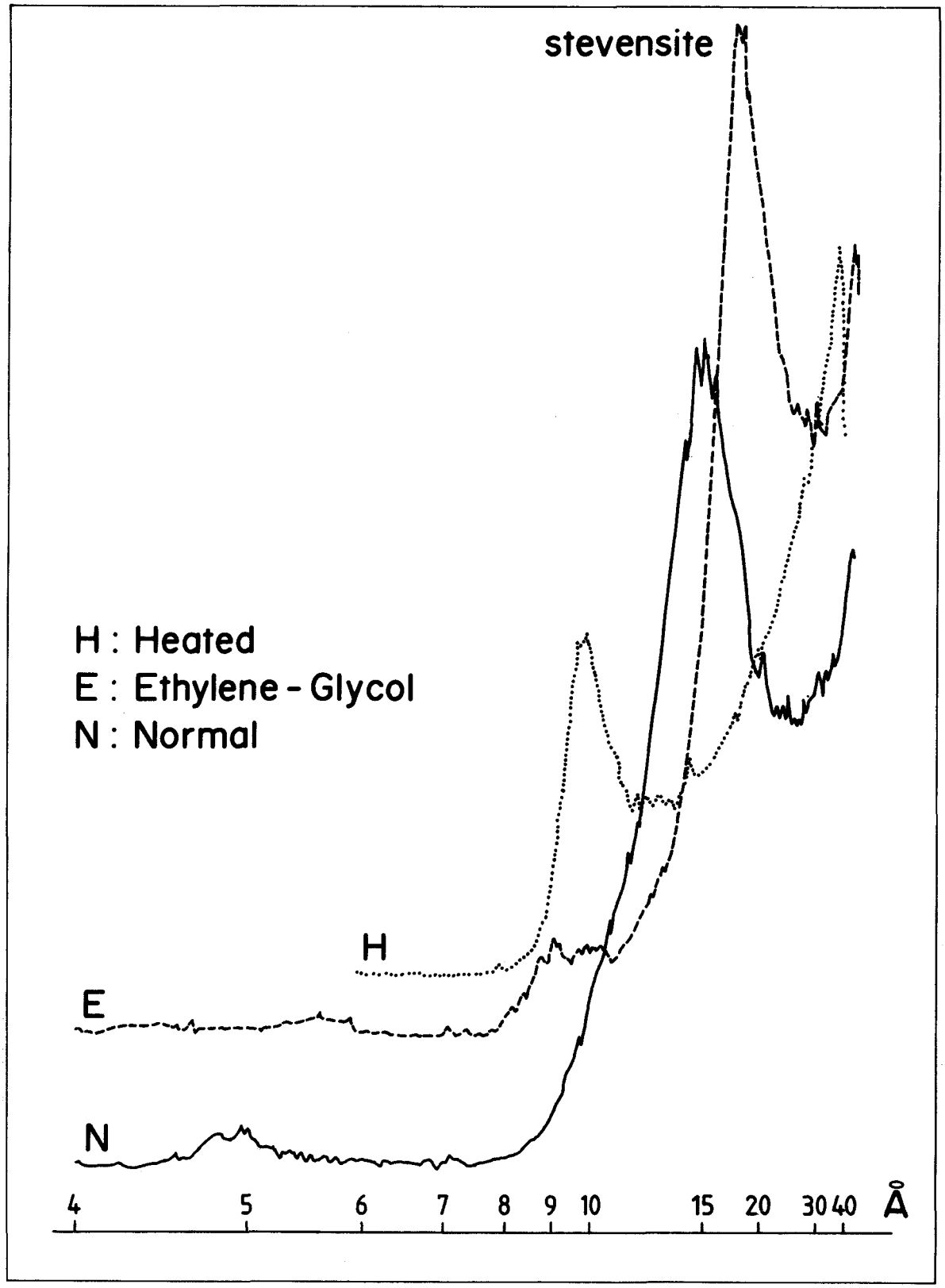

Figure 4. XRD pattern of oriented clays showing stevensite (sample 10).

https://doi.org/10.1346/CCMN.1997.0450308 Published online by Cambridge University Press

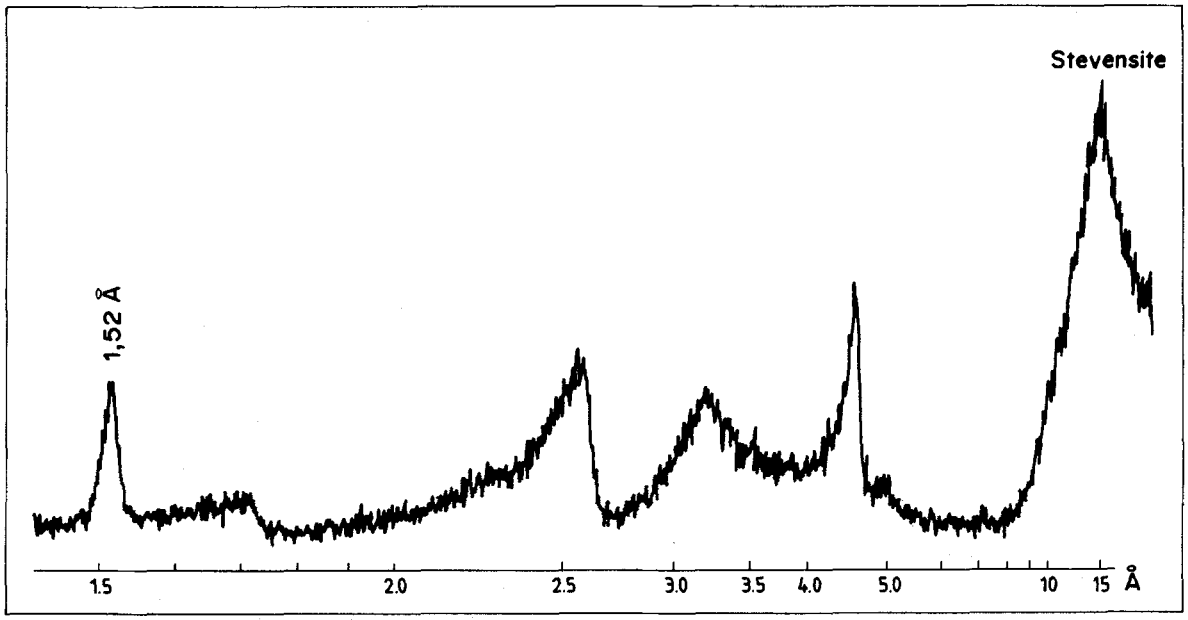

Figure 5. XRD pattern of nonoriented material showing (060) peak of stevensite characteristic of trioctahedral character.

cations; therefore, Fe in stevensite and sepiolite was assumed to be trivalent and attributed to the octahedral sheet.

RESULTS

Mineralogy

The diffraction diagrams show pure stevensite in samples 9, 10 and 11 (Table 2). The stevensite is well crystallized (Figure 4). As *d*(060) is equal to 1.52 Å, it has a trioctahedral character (Figure 5).

Sepiolite is always associated with stevensite. Nevertheless, in sample 7, sepiolite is the dominant clay. Sepiolite is also well ordered (Figure 6). Its peaks (Figure 7) correspond perfectly to the sepiolite in the Joint Committee on Powder Diffraction Standards (JCPDS) index (number 13-595).

We can distinguish the peaks due to stevensite (14 Å) and to sepiolite (12.5 Å). The XRD analyses at atmospheric conditions (N) show assymmetrical peaks either due to stevensite (sample 6), or to sepiolite (sample 8) (Figure 8), depending on the amount of the 2 species.

Major Elements Chemistry

The chemical compositions of the <2 μm fraction of each purified sample are presented in Table 3. The structural formula of pure stevensite (from sample 10), calculated for half-unit cells on the basis of 11 oxygens, is: $(Si_{3.95}Al_{0.05})(Mg_{2.74}Al_{0.07}Fe^{III}_{0.04}Li_{0.09})(Ca_{0.02}Na_{0.02}K_{0.03})O_{10}(OH)_2$. The number of octahedral cations, equal to 2.96 atoms, confirms the trioctahedral character of this stevensite. The latter is Mg-rich with minor amounts of Fe, Al and Li in the octahedral site. The majority of the layer charge is related to the presence of octahedral vacancies. The interlayer cations are K, Ca and Na.

As stevensite and sepiolite are mixed in other samples (6, 7, 8), it was impossible to obtain the composition of each clay species by conventional analytical techniques. Nevertheless, all chemical compositions, especially the composition of sepiolite-rich sample 7, are enriched in Mg and depleted in Li.

Li is never present in the structural formula of natural sepiolites. In some experiments, Mifsud et al. (1987) tried to introduce Li into the octahedral sites of sepiolites; they conclude that the textural, structural and thermal characteristics of the Li-exchanged sepiolite are completely different from those of natural sepiolite. It seems that Li favors the formation of stevensite but inhibits the formation of sepiolite. This may explain the abundance of stevensite and the scarcity of sepiolite in the Jbel Rhassoul sediments, although the dolomitic environment is favorable to sepiolite formation. The same phenomenon seems to occur in Bolivian lakes, where great amounts of stevensite are present, but no sepiolite (Badaut et al. 1979; Badaut and Risacher 1983; Risacher 1992), while the brines are often very rich in Li.

AEM Chemistry

Although sepiolite and stevensite are always mixed in the samples, it was possible to characterize the chemical composition of each of the 2 clay species by electron microprobe techniques.

The stevensite particles occur either as folded layer shapes with rolled up borders, or as flakey shapes.

https://doi.org/10.1346/CCMN.1997.0450308 Published online by Cambridge University Press

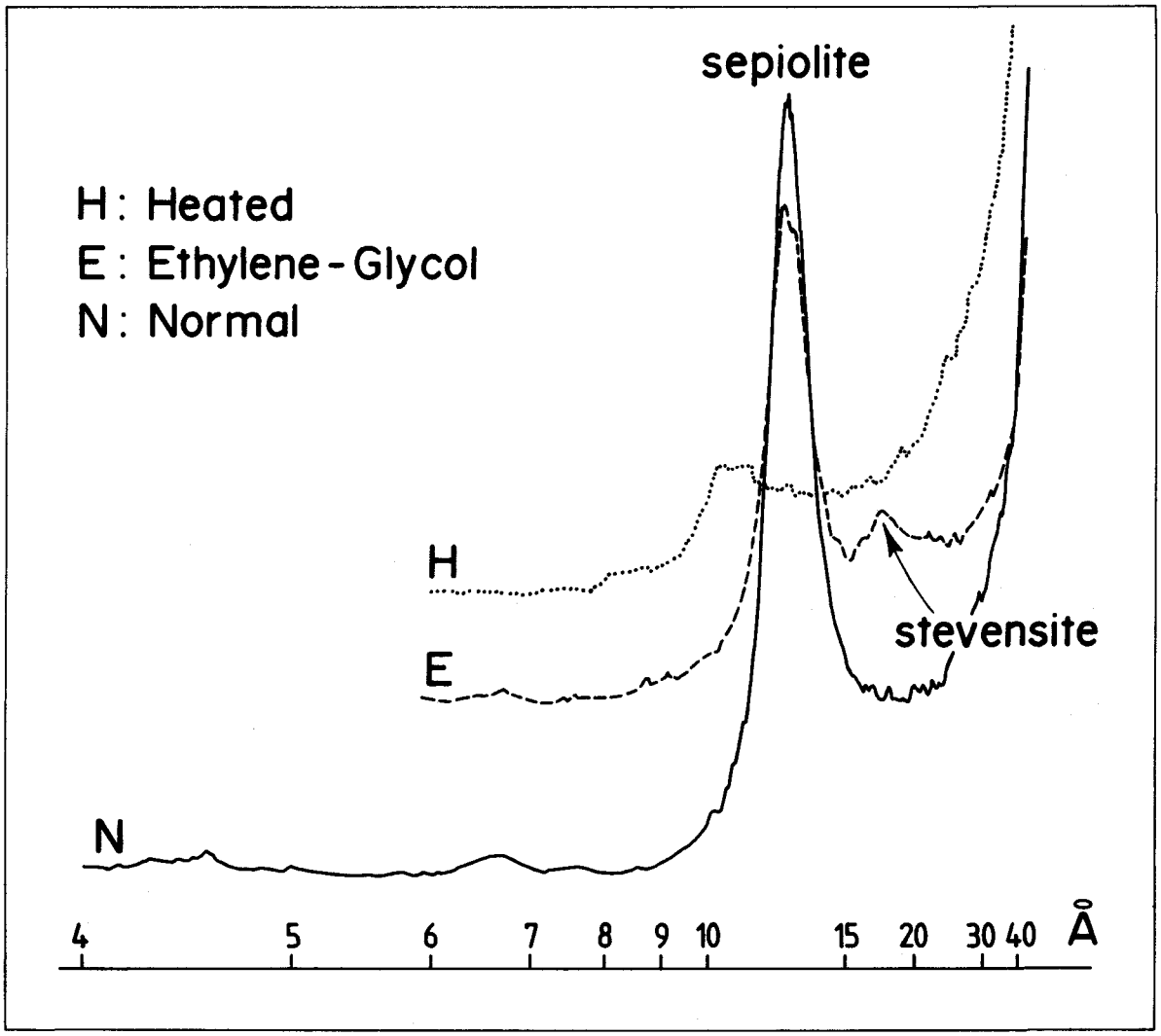

Figure 6. XRD pattern of oriented clays showing sepiolite (sample 7).

They are well crystallized based upon their diffraction pattern and show rings owing to the turbostratic arrangement of the stevensite layers. The mean structural formula of these particles is (for a half-cell): $(Si_4)(Al_{0.21}Fe^{III}_{0.07}Mg_{2.56})Ca_{0.02}O_{10}(OH)_2$. As Li atoms related to the <2 μm fraction are less abundant (about 0.09 atoms), the preceding structural formula could be similar to the Li-bearing formula. The structural formula shows very low interlayer charge and no tetrahedral charge. Magnesium represents 90% and Al 7.5% of the octahedral cations. There are traces of Fe. Although the structural formula of particles and that of the <2 μm fraction show minor differences, both are related to stevensite.

The sepiolite fibers are 10 μm long and often form bundles of a few fibers. The mean structural formula of sepiolite is: $(Si_{5.86}Al_{0.14})(Al_{0.03}Mg_{3.98}Fe^{III}_{0.02})Ca_{0.02}O_{15}(OH)_2 \cdot 6H_2O$. The sepiolite samples studied are Mg-rich with minor amounts of Al and Fe. Their composition is similar to the ideal structural formula of sepiolite (Brauner and Preisinger 1956): $Si_6Mg_4O_{15}(OH)_2 \cdot 6H_2O$.

Texture

In addition to sepiolite with its typical fibrous shape and stevensite with a flake-like texture, numerous other particles show mixed characters. All intermediates exist between stevensite particles having a bristled periphery and showing short needles (Figure 9a) and bundles of few fibers (Figure 9b). These bundles torn off from particles are dispersed and randomly oriented (Figure 9c and 9d). But it is not rare to observe bundles associated in a 120° preferential orientation (Figure 9e). Their electron diffraction pattern, similar to those presented by Caillère et al. (1982) and Wilson (1987), correspond to a well-ordered sepiolite (Figure

https://doi.org/10.1346/CCMN.1997.0450308 Published online by Cambridge University Press

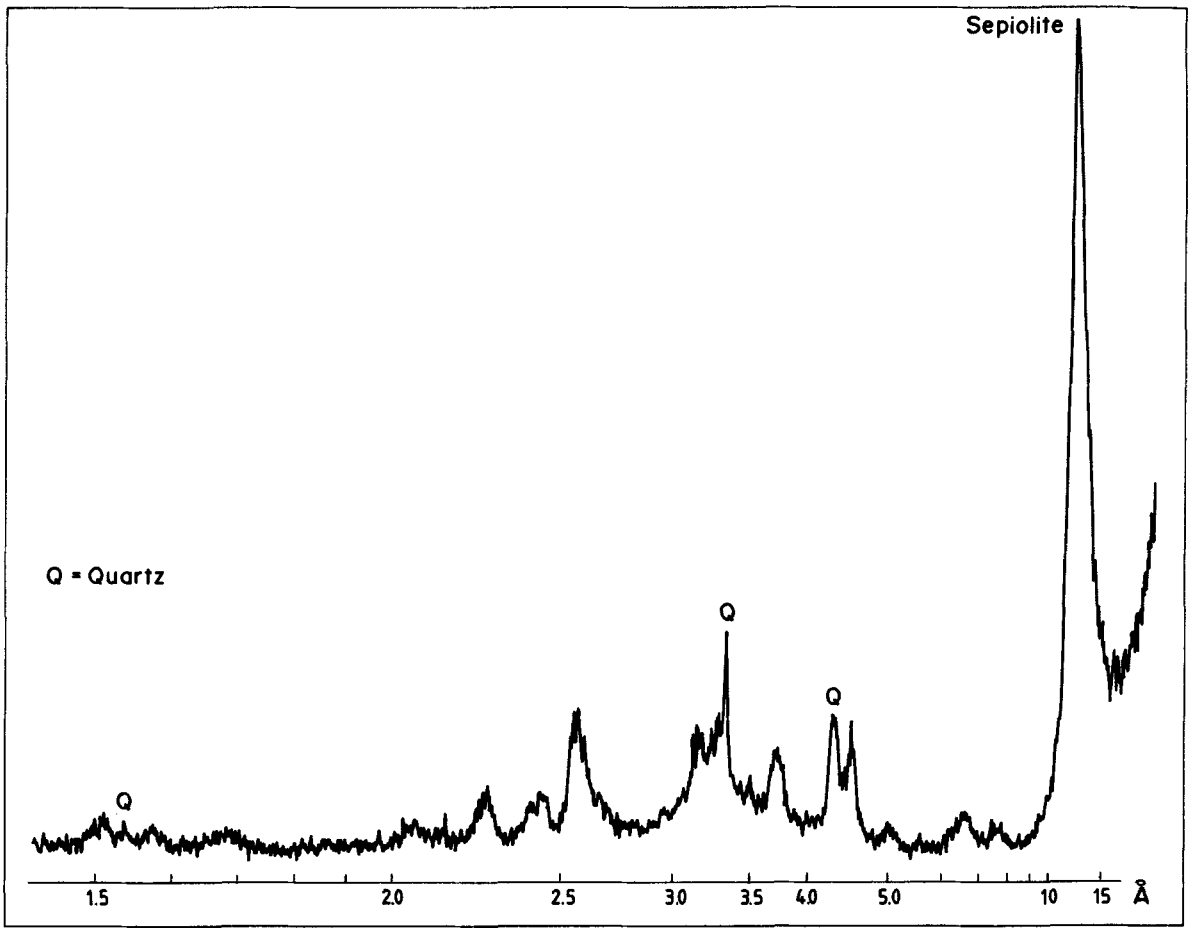

Figure 7. XRD pattern of nonoriented material showing peaks due to sepiolite similar to those in JCPDS index.

Table 3. Chemical composition of the clay species in the <2 μm fractions of the "Formation Intermédiaire" using arc emission spectroscopy.

Sample	11	10	9	8	7	6
SiO_2	59.30	59.30	56.30	58.60	59.40	56.60
Al_2O_3	1.60	1.60	2.90	3.00	1.90	3.20
MgO	26.70	27.40	26.70	22.10	22.90	23.40
CaO	0.40	0.30	0.60	—	—	0.50
Fe_2O_3	0.90	0.90	1.30	1.70	1.00	1.40
Mn_3O_4	—	—	—	—	—	0.01
TiO_2	0.14	0.15	0.16	0.23	0.18	0.21
BaO	—	—	—	—	—	0.01
SrO	—	—	0.05	0.02	0.59	2.16
Na_2O	0.11	0.17	0.12	0.80	0.13	0.08
K_2O	0.46	0.34	0.58	0.74	0.43	0.73
LiO	0.44	0.35	0.29	0.15	0.09	0.35
PF (1000 °C)	10.14	9.50	10.74	12.90	13.68	10.81
Total	100.17	100.10	99.74	101.07	100.41	99.30

Key: PF(1000 °C): loss on ignition; — below detection limit.

https://doi.org/10.1346/CCMN.1997.0450308 Published online by Cambridge University Press

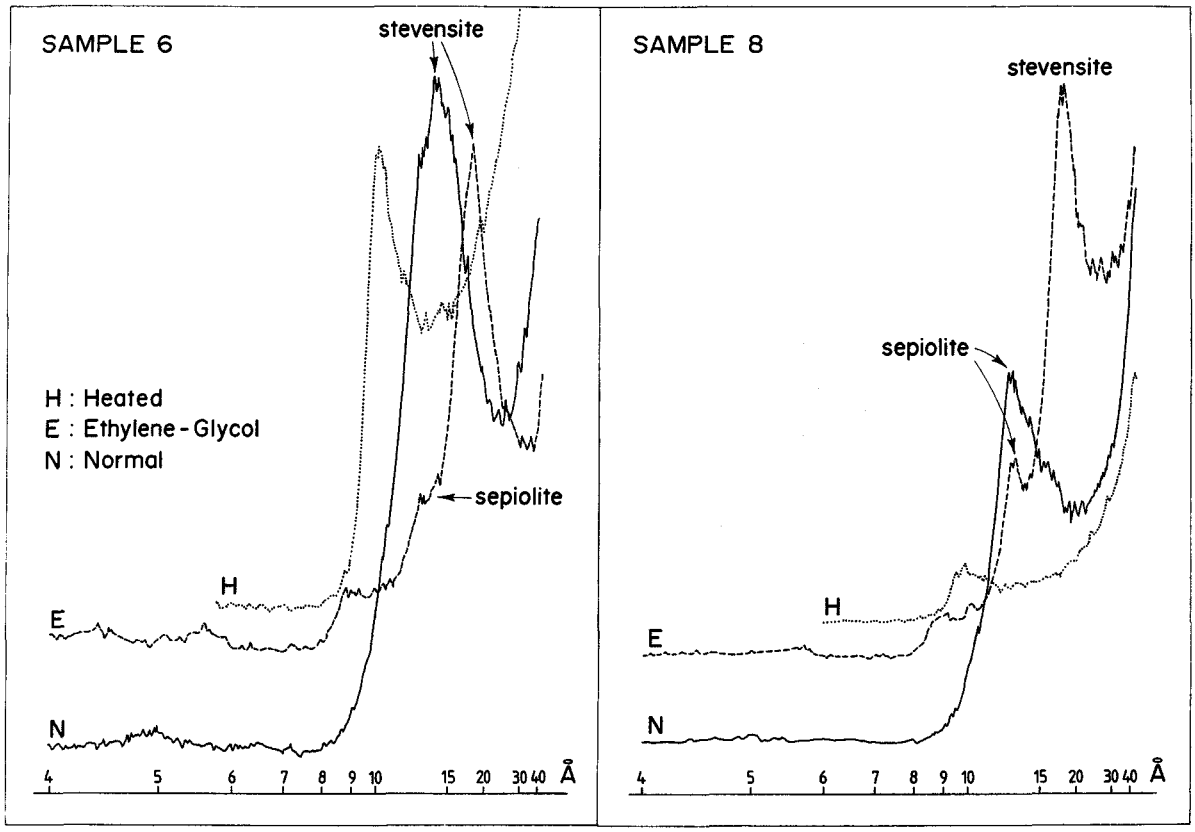

Figure 8. XRD pattern of oriented clays showing stevensite and sepiolite (samples 6 and 8).

9f). We could, of course, determine the sepiolite *d*-value that is equal to 12.5 Å. These TEM observations reveal, clearly, a textural transition between sepiolite and a precursor stevensite. This transition can also be observed by SEM, where the fibers seem to grow at the expense of the stevensite (Figures 9g and 9g'). In high-resolution lattice-fringe images, stevensite particles appear as typically curved and form discontinuous layers (Figure 9h) associated with sepiolite. Hollow arrows indicate cross sections of sepiolite fibers (Figures 9h and 9h').

To our knowledge, such TEM observations are uncommon. Nevertheless, according to Khoury et al. (1982), SEM images show sepiolite growing from stevensite. Doval et al. (1987) also present a genetic relationship between smectite and sepiolite by means of SEM observations.

The textural transition suggests a secondary origin of sepiolite that forms on a stevensite substrate.

Trace Elements Chemistry

Three samples were selected for trace elements analyses: 1 rich in stevensite (9), another in sepiolite (7) and mixed stevensite and sepiolite (8). Except for Zr and Cr, the distribution of trace elements (Figure 10) is similar in all samples (that is, for stevensite and sepiolite). That means that the stevensites and sepiolites may have either formed together from the same

Table 4. Dissolution reactions and log K values at 25 °C of minerals used for thermodynamic calculations.

Name	Source	Dissolution reaction	log K
Ca-stevensite	1	$(Si_{4.00}Mg_{2.9}O_{10}(OH)_2Ca_{0.1}) + 6H^+ + 4H_2O = 4H_4SiO_4 + 2.9Mg^{2+} + 0.1Ca^{2+}$	25.45
Kerolite	2	$(Si_{4.00}Mg_{3.0}O_{10}(OH)_2) + 6H^+ + 4H_2O = 4H_4SiO_4 + 3Mg^{2+}$	25.79
Sepiolite	3	$(Si_{6.00}Mg_{4.0}O_{15}(OH)_26H_2O) + 8H^+ + H_2O = 6H_4SiO_4 + 4Mg^{2+}$	31.00

1) This work, log K (25 °C) has been calculated by means of the solid-solution model described by Fritz (1981) and Tardy and Fritz (1981).
2) Stoessel (1988).
3) Helgeson et al. (1978).

https://doi.org/10.1346/CCMN.1997.0450308 Published online by Cambridge University Press

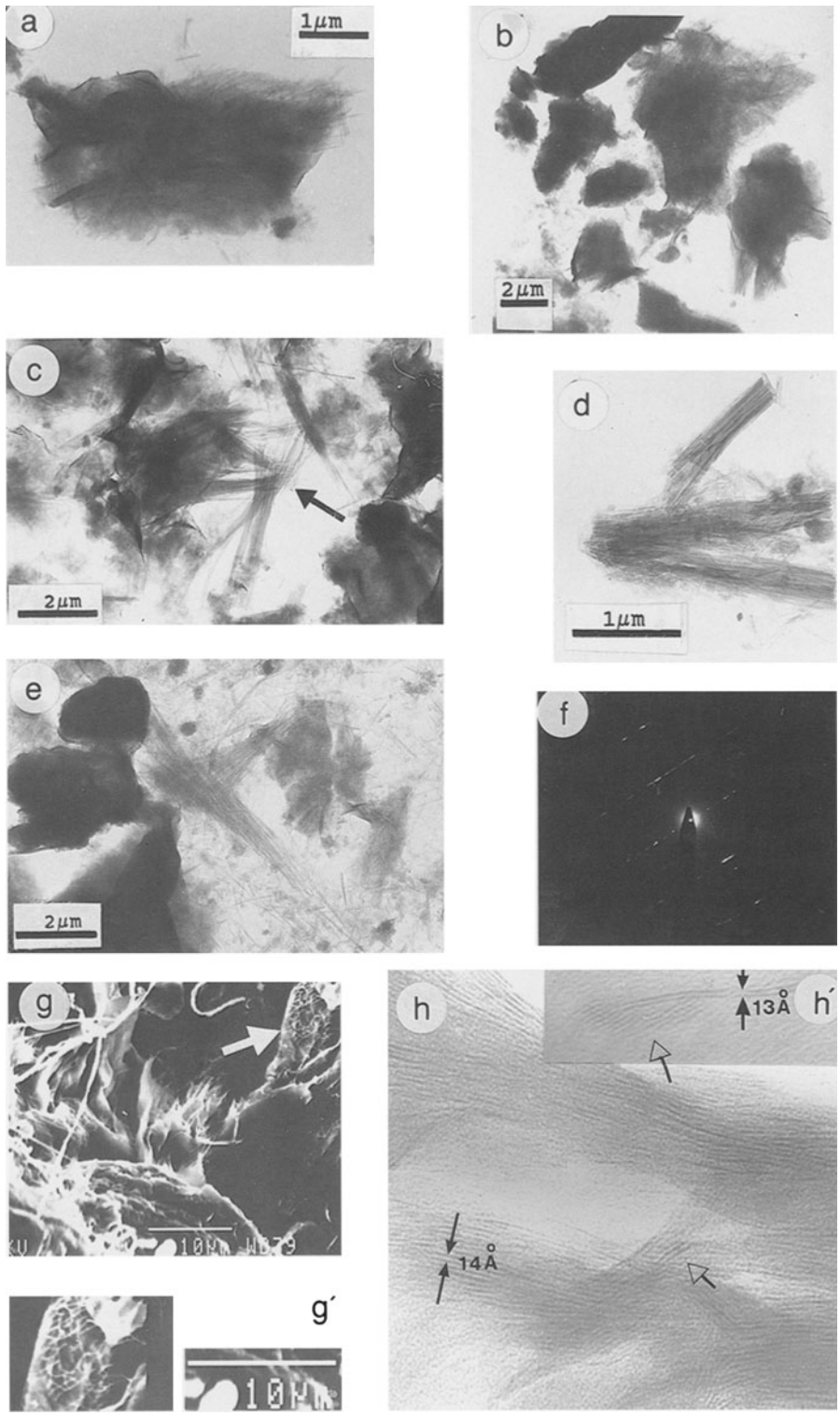

Figure 9. a) Stevensite particles having a bristled periphery with short and closed needles. b) Stevensite particles with bundles of a few fibers. c) Bundles of fibers torn off from particles. d) Bundles of fibers dispersed and randomly oriented. e) Bundles of 120°-oriented fibres. f) Electron diffraction pattern of a sepiolite similar to those realized by Caillère et al. (1982) and Wilson (1987) showing a well-crystallized sepiolite. g) and g′) Sepiolite fibers seem to grow at the expense of stevensite particles. h) High-resolution lattice-fringe image of stevensite particles showing typically curved and discontinuous layers. h') Sepiolite is associated with stevensite: arrows indicate a cross section of fibers.

https://doi.org/10.1346/CCMN.1997.0450308 Published online by Cambridge University Press

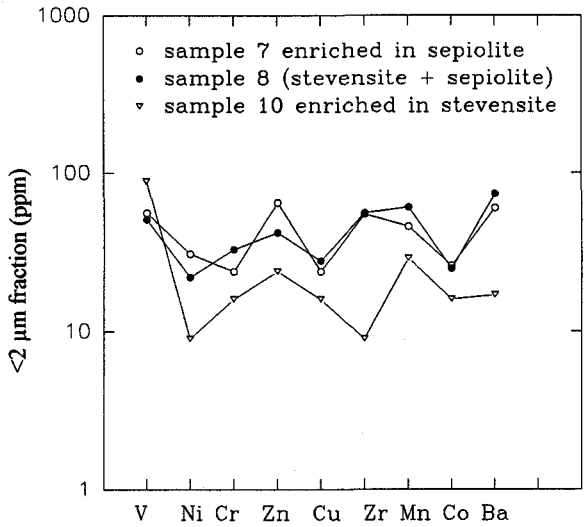

Figure 10. Trace element distribution in stevensite (sample 10), sepiolite (sample 7) and in the mixture of stevensite and sepiolite (sample 8).

environment, or as a generation, one from the other with enrichment of Zr, impoverishment of Cr and without loss of other trace elements. The textural transition between precursor stevensite and sepiolite confirms this latter hypothesis.

Geochemical Conditions for the Formation of Sepiolite after Stevensite

Our main purpose was to establish low-temperature stability fields for standard stevensite (Ca-stevensite) and standard sepiolite, and subsequently to determine the geochemical conditions favorable for the formation of sepiolite after stevensite. Although kerolite is not found in Jbel Rhassoul sediments, it is often associated with sepiolite. A stability field diagram was established for the stevensite–sepiolite–kerolite system at 25 °C. The different log K values at 25 °C are given in Table 4. The interrelations between stevensite, sepiolite, kerolite and aqueous solution at 25 °C are shown in terms of log $[Mg^{2+}]/[H^+]^2$ and log $[H_4SiO_4]$. The Tertiary paleogeography of the Jbel Rhassoul region was considered as similar to that of present days (Ais 1984); thus we consider that the chemical composition of the meteoric waters draining the dolomite-rich Jurassic-Cretaceous formations of Jbel Rhassoul hinterland may have been similar to those that filled the lake where stevensite was formed after dolomite (Chahi 1996). On this basis, we have fixed log $([Ca^{2+}]/[H^+]^2)$ at 12.8 (log $[Ca^{2+}] = -3.1$, pH = 7.95 in diluted water undersaturated with dolomite).

As shown on Figure 11, the increase of silica and Mg activities from the solution leads the reaction path

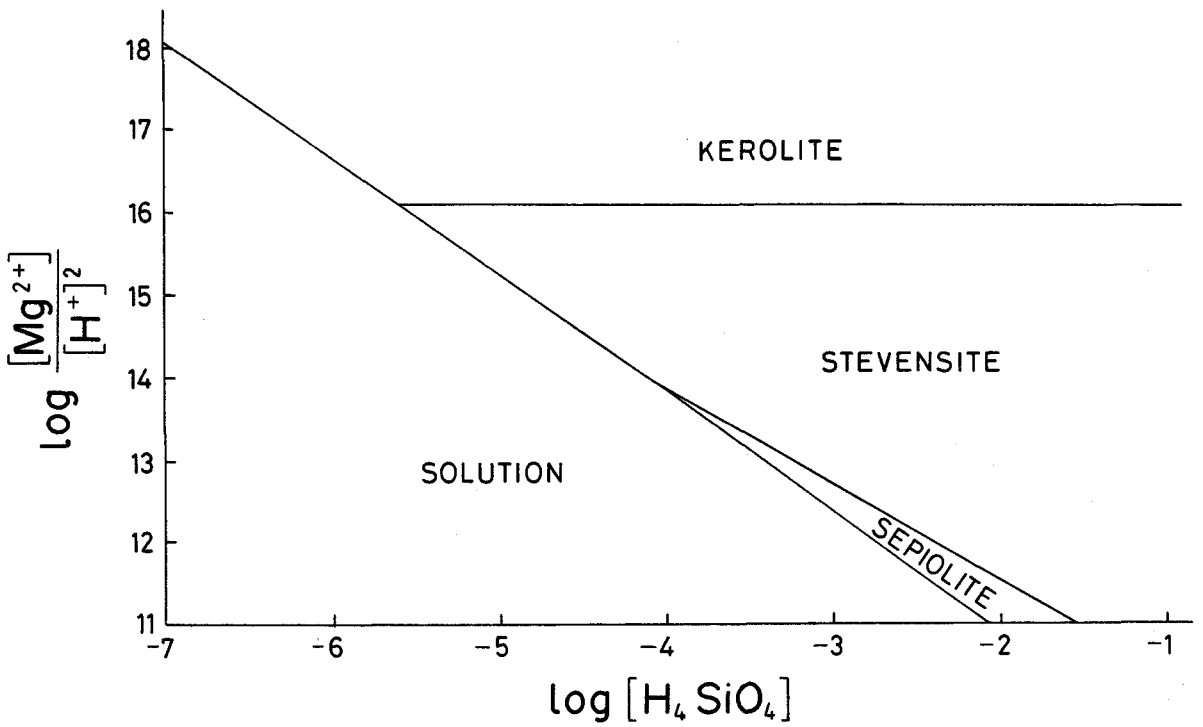

Figure 11. Stability fields of standard sepiolite, Ca-stevensite, kerolite and aqueous solution at 25 °C, at log $([Ca^{2+}]/[H^+]^2) = 12.8$.

https://doi.org/10.1346/CCMN.1997.0450308 Published online by Cambridge University Press

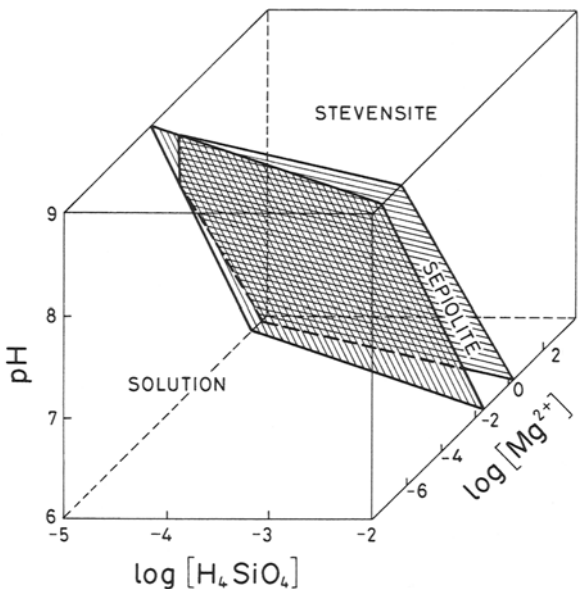

Figure 12. Stability fields of standard sepiolite, Ca-stevensite and aqueous solution at 25 °C, log $[Ca^{2+}] = -3.1$.

into the kerolite or stevensite field at higher pH, whereas at lower pH the reaction path evolves to the sepiolite field.

Dissolution of stevensite lead to equilibrium between stevensite and the silica- and Mg-poor solution. However, at higher pH, dissolution of stevensite in the relatively Mg-rich solution leads to formation of kerolite, because the Si/Mg ratio in kerolite is lower than in stevensite (Figure 11). Alternatively, at lower pH, dissolution of stevensite in the relatively silica-rich solution leads to formation of sepiolite, because the Si/Mg ratio in sepiolite is higher than in stevensite, and sepiolite is not stable at low silica concentration (Figures 11 and 12).

DISCUSSION AND CONCLUSIONS

There have been 2 main mechanisms of sepiolite formation reported. The 1st is neoformation by evaporation. Several authors, among others Trauth (1977), consider that sepiolite is a siliceous evaporite. The 2nd mechanism is dissolution-crystallization during diagenesis. Many authors describe such a mechanism, as for example Eberl et al. (1982) and Khoury et al. (1982), who suggest that sepiolites crystallize after dissolution of kerolite/stevensite. In the case of the "Ballarat" formation in California, Post and Janke (1984) think that it is altered saponite that provides Mg and Si necessary for the formation of sepiolite. The same is true for sepiolite in the fluvio-lacustrine environment of the Neogene basin from Madrid (Leguey et al. 1985). In the Pleistocene deposits of Tecopa Lake in southeast California, detrital smectites brought by the Amargosa River may have been the clay precursors for sepiolite (Jones and Galan 1988). In the Jbel Rhassoul, textural arguments plead for a mechanism of formation by destabilization and transformation of a precursor stevensite. Our study, in conjunction with previous works on the Jbel Rhassoul deposits, suggests a possible scenario for the formation of the Jbel Rhassoul sepiolite in the Tertiary lacustrine environment.

Sepiolite occurs stratigraphically between the upper part of the "Formation Intermédiaire", which is rich in stevensite, and the "Formation Rouge", which is rich in palygorskite. The "Formation Rouge" formed in a playa environment under a dry climate (Chahi, Duplay and Lucas 1993; Gautier-Lafaye et al. 1993; Duringer et al. 1995; Chahi 1996), whereas stevensite formed in a perennial lake under a wet climate by dissolution of dolomite with excess silica provided by dissolution of diatom frustules (Chahi et al. 1992; Duringer et al. 1995; Chahi 1996). Thus, sepiolite formed under climatic conditions varying between dry and wet during the early development of the lacustrine system that led to the deposition of the "Formation Intermédiaire". Because the perennial wet climate led to the formation of pure mineable beds of stevensite without any trace of sepiolite, the sepiolite may be formed under dry climatic periods. During these periods, the relative enrichment in silica and the pH decrease of the lake water destabilized the stevensite, leading to the formation of sepiolite. The dry episodes never lasted long enough to completely alter the stevensite.

ACKNOWLEDGMENTS

The authors wish to acknowledge R. K. Stoessel and D. Eberl for their critical review of this paper.

REFERENCES

Ais M. 1984. Etude géologique du gisement de rhassoul de Tamdafelt (bassin de Missour) [M.S. Thesis]. Fes, Morocco: Univ Sidi Mohamed Ben Abdelah. 31 p.

Badaut D, Risacher F. 1983. Authigenic smectite on diatom frustules in Bolivian saline lakes. Geochim Cosmochim Acta 47:363–375.

Badaut D, Risacher F, Paquet H, Eberhart JP, Weber F. 1979. Néoformation de minéraux argileux à partir de frustules de diatomées: le cas des lacs de l'Altiplano bolivien. CR Acad Sci Paris, Ser D 289:1191–1193.

Brauner K, Preisinger A. 1956. Struktur und Entschung des sepioliths. Tschermaks Min Petr Mitt 6:120–140.

Caillère S, Henin S, Rautureau M. 1982. Minéralogie des argiles. Paris: Masson. 184 p.

Chahi A. 1988. Recherche de quelques méthodes de purification des minéraux argileux. Etude cristallochimique de quelques échantillons du Jbel Rhassoul [M.S. thesis]. Strasbourg, France: Univ Louis Pasteur. 30 p.

Chahi A. 1992. Comparaison des minéraux argileux des formations lacustres du Jbel Rhassoul et des phosphorites marines des Ganntour au Maroc. Genèse des minéraux argileux magnésiens [thèse de doctorat]. Strasbourg, France: Univ Louis Pasteur. 211 p.

Chahi A. 1996. Les minéraux argileux des gisements de phosphorites des Ganntour et de stévensite du Jbel Rhas-

soul (Maroc): relations génétiques entre les argiles 2:1 et les argiles fibreuses en conditions de surface [thèse de doctorat d'état es. sciences]. Marrakech: Univ Cadi Ayyad. 166 p.

Chahi A, Duplay J, Lucas J. 1993. Analyses of palygorskite and associated clays from the Jbel Rhassoul (Morocco): Chemical characteristics and origin of formation. Clays Clay Miner 41:401–411.

Chahi A, Risacher F, Ais M, Duringer P. 1992. Diagenetic stevensite after dolomite in lacustrine deposit of Jbel Rhassoul (Morocco). In: Karaka YK, Maest AS, editors. Proc Int Symp water rock interaction: Park City, UT. Rotterdam: Balkema. p 627–629.

Chahi A, Weber F, Prévôt L, Lucas J. 1993. L'utilisation des résines échangeuses de cations (Amberlite IRC-50H) dans la dispersion et la purification des roches à carbonates, phosphates et sulfates. Clay Miner 28:585–601.

Cliff G, Lorimer GW. 1975. The quantitative analysis of thin specimens. J Microsc 103:203–207.

Doval M, Rautureau M, Brell JM, Fontaine C. 1987. Cristalchemistry of "pink clays" from the Tertiary Madrid Basin. Its relationship with the sepiolite occurrence. In: Galan E, Perez-Rodriguez J, Cornejo J, editors. Proc 6th Meet Euro Clay Groups; Seville, Spain. p 203–204.

Duplay J. 1988. Géochimie des argiles et géothermométrie des populations monominérales de particules [thèse de doctorat d'état es. sciences]. Strasbourg: Univ Louis Pasteur. 222 p.

Duringer P, Ais M, Chahi A. 1995. Contexte géodynamique et milieu de dépôt du gisement de stévensite (rhassoul) miocène du Maroc: Environnement lacustre ou évaporitique? Bull Soc Geol Fr 166:169–179.

Fritz B. 1981. Etude thermodynamique et modélisation des réactions hydrothermales et diagénétiques. Sci Geol Mémoire 65. 197 p.

Gauthier-Lafaye F, Taieb R, Paquet H, Chahi A, Prudencio I, Sequeira Braga MA. 1993. Composition isotopique de l'oxygène de palygorskites associées à des calcrètes: conditions de formation. CR Acad Sci Paris, t316:1239–1245.

Hay RL, Stoessell RK. 1984. Sepiolite in the Amboseli Basin of Kenya: A new interpretation. In Singer A, Galan E, editors. Palygorskite–sepiolite: Occurrences, genesis and uses. Dev Sedimentol 37. Amsterdam: Elsevier. p 125–136.

Helgeson HC, Delany JM, Nesbitt HW, Bird DK. 1978. Summary and critique of the thermodynamic properties of rock-forming minerals. Am J Sci 278:1–229.

Jones BF, Galan E. 1988. Sepiolite and palygorskite. In Bailey SW, editor. Hydrous phyllosilicates. Rev Mineral 19. Washington, DC: Mineral Soc Am. p 631–667.

Khoury HN, Eberl DD, Jones BF. 1982. Origin of magnesium clays from the Amargosa Desert, Nevada. Clays Clay Miner 30:327–336.

Leguey S, Pozo M, Medina JA. 1985. Polygenesis of sepiolite and palygorskite in a fluvio-lacustrine environment in the Neogene Basin of Madrid. Miner Petrogr Acta 29:287–301.

Lucas J, Prévôt L. 1976. Etude géologique du gisement du rhassoul de Tamdafelt (Ksabi). Rapport interne de Institut de Géologie, Strasbourg. 16 p

McLean SA, Allen BL, Craig JR. 1972. The occurence of sepiolite and attapulgite on the southern High Plains. Clays Clay Miner 20:143–149.

Mifsud A, Garcia I, Corma A. 1987. Thermal stability and textural properties of exchanged sepiolites. In Galan E, Perez-Rodriguez J, Cornejo J, editors. Proc 6th Meet Euro Clay Groups; Sevilla, Spain. p 392–394.

Papke KG. 1972. A sepiolite-rich playa deposit in southern Nevada. Clays Clay Miner 20:211–215.

Parry WT, Reeves CC. 1966. Lacustrine glauconitic mica from pluvial Lake Mound, Lynn and Terry Countries, Texas. Am Miner 51:229–235.

Peacor DR. 1992. Analytical electron microscopy: X-ray analysis. In Buseck PR, editor. Minerals and reactions at the atomic scale. Transmission electron microscopy. Rev Mineral 27. Mineral Soc Am. p 113–140.

Post JL, Janke NC. 1984. Ballarat sepiolite, Inyo County, California. In Singer A, Galan E, editors. Palygorskite–sepiolite: Occurrences, genesis and uses. Dev Sedimentol 37. Amsterdam: Elsevier. p 159–168.

Raynal R. 1952. Quelques données nouvelles au sujet de l'Oligo-Miocène du bassin de la Moulouya. CRS Soc Geol Fr 6:43–44.

Risacher F. 1992. Géochimie des bassins à évaporites de l'Altiplano bolivien [thèse de doctorat]. Strasbourg, France: Univ Louis Pasteur. 233 p.

Samuel J, Rouault R, Besnus Y. 1985. Analyse multiélémentaire standardisée des matériaux géologiques en spectrométrie d'émission par plasma à couplage inductif. Analusis 17:312–317.

Stoessell RK. 1988. 25 °C and 1 atm dissolution experiments of sepiolite and kerolite. Geochim Cosmochim Acta 52: 365–374.

Stoessell RK, Hay RL. 1978. The geochemical origin of sepiolite and kerolite at Amboseli, Kenya. Contrib Mineral Petrol 65:255–267.

Tardy Y, Fritz B. 1981. An ideal solid solution model for calculating solubility of clay minerals. Clay Miner 16:361–373.

Trauth N. 1977. Argiles évaporitiques dans la sédimentation carbonateé continentale et épicontinentale tertiaire. Bassin de Paris, de Mormoiron et de Salinelles (France) et du Jbel Ghassoul (Maroc). Sci Geol Mémoire 49. 195 p.

Wilson MJ. 1987. A handbook of determinative methods in clay mineralogy. Glasgow and London: Blackie. 308 p.

(Received 10 May 1994; accepted 5 July 1996; Ms. 2506)